

Journal of Mechanics of Materials and Structures

**ELASTIC MODULI OF BORON NITRIDE NANOTUBES BASED
ON FINITE ELEMENT METHOD**

Hossein Hemmatian, Mohammad Reza Zamani and Jafar Eskandari Jam

Volume 13, No. 3

May 2018



ELASTIC MODULI OF BORON NITRIDE NANOTUBES BASED ON FINITE ELEMENT METHOD

HOSSEIN HEMMATIAN, MOHAMMAD REZA ZAMANI AND JAFAR ESKANDARI JAM

Boron nitride nanotubes (BNNTs) possess superior thermal conductivity and mechanical/electrical properties, and are a suitable and favourable reinforcement for nanocomposites. Experimental studies on nanoscale materials are time-consuming, costly, and require accurate implementation. Therefore, a three-dimensional finite element (FE) model of a space-frame structure is proposed for BNNTs, which is based on molecular structural mechanics. The effects of length, chirality, diameter, and defect on the elastic moduli of BNNTs are investigated. The results show that defects in the nanotubes decrease the mechanical properties. The values of the Young's modulus and shear modulus of BNNTs without defects change from 1.022 TPa to 1.042 TPa and from 0.33 TPa to 0.536 TPa, respectively. It is found that, with increasing chirality and radius of BNNTs, the Young's modulus and shear modulus increase. As the length of zigzag and armchair BNNTs increases, the Young's modulus increases and the shear modulus decreases. Also, it was observed that by using the finite element method (FEM) based on molecular dynamics, one can accurately determine the mechanical properties of BNNTs. The results demonstrate that the proposed FE model is a valuable tool for studying the mechanical behaviour of BNNTs.

1. Introduction

Rubio et al. [1994] theoretically predicted boron nitride nanotube (BNNT). Then, Chopra et al. [1995] synthesized double-walled boron nitride nanotube (DWBNT), and afterwards single-walled boron nitride nanotube (SWBNT) was produced by arc discharge [Loiseau et al. 1996] and chemical substitution reactions [Golberg et al. 1999]. Over the past two decades, BNNTs have attracted researchers attention in different fields due to their novelty and superlative mechanical [Chen et al. 2004b; Griebel and Hamaekers 2007; Vaccarini et al. 2000], electrical [Khoo et al. 2004; Chen et al. 2004a; Ishigami et al. 2005; Terrones et al. 1996], and chemical properties [Golberg et al. 2001].

Similar to carbon nanotubes (CNTs), a BNNT can be imagined as rolled up hexagonal BN layers and have different types chirality, as well as zigzag and armchair configurations [Chopra et al. 1995]. BNNTs, like CNTs, have extraordinary mechanical properties [Hernández et al. 1998; Chopra and Zettl 1998], high thermal conductivity along the nanotube length [Chang et al. 2005], and good resistance to oxidation at high temperature [Chen et al. 2004b]. Despite their similar structures, BNNTs have different properties because of their different atoms [Fereidoon et al. 2015]. CNTs show a metallic, semiconductor, or insulator characteristic depending on chirality and diameter, while BNNTs, independent of their chirality, diameter, and number of walls, behave as an insulator for low electric fields [Khaleghian and Azarakhshi 2016; Molani 2017].

Keywords: elastic moduli, boron nitride nanotube, chirality, length, finite element method.

In addition, BNNTs are better able to store hydrogen compared to CNTs and have found many applications in hydrogen storage [Wu et al. 2004]. BNNTs are also nontoxic to health and environment due to their chemical inertness and structural stability. Therefore, BNNTs are particularly suitable for biological employment [Zhi et al. 2005].

The elastic properties of BNNTs have theoretically and experimentally been investigated. Slightly different results were presented, but all calculated values indicate a very high Young's modulus (note that it is slightly smaller than for CNTs), which has led to their use as a structural reinforcement of matrix materials [Zhi et al. 2010]. Polymer nanocomposites combining polymers and nanofiller components have attracted research attention from the academic and industrial communities due to their diverse functional applications, good processing, and relatively low cost [Mehar et al. 2017b; 2018].

First-principles [Bahrami Panah and Vaziri 2015], tight-binding [Hernández et al. 1998], density functional [Mirzaei and Salamat Ahangari 2016], and classical molecular mechanics [Li and Chou 2006] approaches have been performed to characterize the properties of BNNTs. By using thermal vibration amplitude analysis, Chopra and Zettl [1998] estimated $1.22 \text{ TPa} \pm 0.24 \text{ TPa}$ for the Young's modulus of multiwalled boron nitride nanotubes (MWBNNNTs). Hernández et al. [1999] employed the tight-binding method to obtain 862 GPa–940 GPa for the axial Young's modulus of BNNTs. Verma et al. [2007] obtained the axial Young's modulus of the zigzag and armchair BNNTs using the tight-binding method. They also observed that the Young's modulus of zigzag tubes is higher than for armchair ones.

Akdim et al. [2003] indicated that the Young's modulus of BNNTs is in range of 0.71 TPa–0.83 TPa and is slightly dependent on the tube diameter. Also, theoretically, Young's modulus has been predicted to be 1.2 TPa [Hernández et al. 1998; 1999].

The Young's modulus of DWBNNT was calculated by Fakhrabad and Shahtahmassebi [2013] using the ab initio calculations based on density functional theory (DFT), and their estimated value is 821 GPa and 764 GPa for $(2, 2) @ (7, 7)$ and $(2, 2) @ (9, 9)$, respectively. The Young's modulus of SWBNNTs with vacancy and functionalization defects was calculated by Gerible and Hamaekers [Griebel et al. 2009] using a molecular dynamics (MD) simulation. They found that Young's modulus decreases with increasing defect concentration. Furthermore, for functionalized BNNTs, they reported no significant decrease with increasing functionalization [Santosh et al. 2009].

The experimental value of Young's modulus of BNNTs is reported to be 1.1 TPa–1.3 TPa [Bettinger et al. 2002]. In another experimental effort, Wei et al. [2010] obtained the value of 895 GPa for the Young's modulus of MWBNNT. Suryavanshi et al. [2004] applied the electric-field-induced resonance method and specified the Young's modulus as 0.8 TPa. Golberg et al. [2007] used an integrated TEM-atomic force microscope (AFM) piezodriven holder to directly test the elastic modulus. The values of 0.5 TPa–0.6 TPa were found for MWBNNTs grown by the BOCVD method.

Experimental studies on nanoscale materials are time-consuming, costly, and require accurate implementation. Therefore, analytical, computational, and theoretical approaches are applied to predict the mechanical properties of nanoscale materials [Mehar et al. 2017a; 2017c; 2017d; Mehar and Panda 2017]. Two main classes of theoretical methods are the atomistic-based methods [Yakobson et al. 1996; Lu 1997; Sánchez-Portal et al. 1999] and the continuum mechanics-based ones [Li and Chou 2003; Chang and Gao 2003; Odegard et al. 2002]. A three-dimensional finite element (FE) model, named as the space-frame model, is used to study the mechanical behaviour of BNNTs. Ansari et al. [2015] used DFT calculations to obtain accurate force constants which are employed when determining element properties.

Fundamental to these approaches, BNNTs are considered as geometrical space-frame structures. Therefore, BNNTs can be analysed by classical structural mechanics. In this paper, the effects of length, chirality, diameter, and defect on the elastic moduli of BNNTs are studied. While this method is conceptually simple and computationally efficient, our results indicate that its computational accuracy is comparable to that of more refined methods such as first-principle and tight-binding methods. Our study has clearly demonstrated the dependency of Young's modulus and shear modulus of BNNTs on tube length, chirality, and radius.

2. FE modelling

2.1. Atomic structure of BNNTs. The atomic structure of BNNTs depends on chirality, which is defined by the chiral vector \vec{C}_h and the chiral angle θ . The chiral vector \vec{C}_h can be defined in terms of the lattice translation indices (n, m) and the basic vectors \vec{a}_1 and \vec{a}_2 of the hexagonal lattice as [Hemmatian et al. 2014]

$$\vec{C}_h = n\vec{a}_1 + m\vec{a}_2. \quad (1)$$

The chiral angle θ is the angle between the chiral vector \vec{C}_h with respect to the zigzag direction $(n, 0)$ where $\theta = 0^\circ$. For the chiral angles of 0° and 30° , the armchair and zigzag nanotubes are formed, respectively. In terms of the roll-up vector, the armchair nanotubes are defined by (n, n) and the zigzag nanotubes by $(n, 0)$. For chiral angles different from 0° and 30° , the chiral nanotubes, which are defined by a pair of indices (n, m) , where $n \neq m$, are formed. Schematic representations of the three types of nanotubes are shown in Figure 1.

2.2. Modelling. BNNTs atoms are bonded together with covalent bonds forming a hexagonal lattice. These bonds have a characteristic bond length and bond angle in the 3D space. The displacement of individual atoms under an external force is constrained by the bonds. Therefore, the total deformation of the nanotube is the result of the interactions between the bonds. By considering the bonds as connecting load-carrying elements, and the atoms as joints of the connecting elements, BNNTs may be simulated as space-frame structures and their mechanical behaviour can be analysed using classical structural mechanics. The 3D FE model is developed using the ANSYS commercial code to assess the mechanical properties of BNNTs.

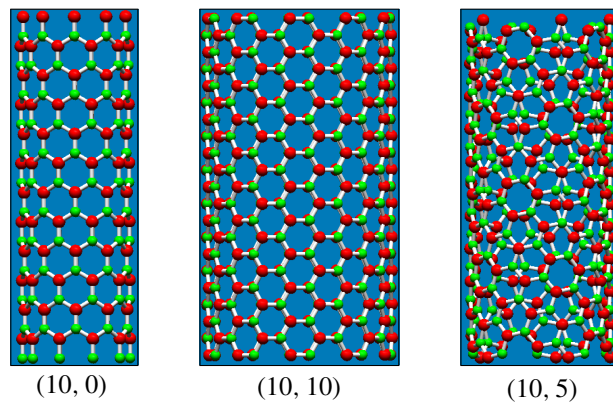


Figure 1. Schematic diagram of zigzag (10, 0), armchair (10, 10), and chiral (10, 5) nanotubes.

| | |
|---|--|
| nanotube diameter, d | 1.648 Å |
| cross-sectional area, A | 2.132 Å ² |
| length of boron-nitrogen bond, l | 1.45 Å |
| polar inertia momentum, I_{xx} | 0.7250 Å ⁴ |
| inertia momentum, $I_{zz} = I_{yy} = I$ | 0.3625 Å ⁴ |
| Young's modulus, E | 4.2155 · 10 ⁻⁸ N/Å ² |
| shear modulus, G | 4.9437 · 10 ⁻⁹ N/Å ² |

Table 1. The properties of beam elements for a real BNNT [Ansari et al. 2015].

To model a BNNT, it is necessary to create atomic coordinates in the form of a keypoint or node and connecting atoms by a line or element. One of the possible outputs of the Nanotube Modeller software is the PDB, which specifies the coordinates of each atom as x , y , and z , and also identifies the connected atoms. But this output is not understandable for ANSYS, which is an APDL programming language. To convert the output file of the PDB format into an APDL language, Python interface programming software is used. A brief program in Python is written for each atom of carbon, a point with coordinates x , y , and z , and for each atomic connection, which creates a line between the two points. The 3D elastic BEAM4 element is used for meshing lines and modelling bonds. This element is a uniaxial element with tension, compression, torsion, and bending capabilities. It has six degrees of freedom at each node: translations in the nodal x -, y -, and z -directions and rotations about the nodal x -, y -, and z -axes. The element is defined by two or three nodes as well as its cross-sectional area, two moments of inertia, two dimensions, and the material properties. For the automatic generation of the BN bonds elements, a routine was created using the ANSYS macrolanguage.

2.3. Atomic properties of beam elements. Molecular structural mechanics (MSM) along with FEM is used for modelling. MSM is a moderately new technique for the mechanical modelling of nanostructures [Li and Chou 2003]. Covalent bonds are modelled with beam elements as they form only at certain intervals among atoms and act linearly. The properties of these elements are obtained by linking the potential energy of bonds (from a chemical point of view) and the strain energy of mechanical elements (from a mechanical point of view). To represent the covalent bond between boron and nitrogen atoms, a circular beam of length l , diameter d , Young's modulus E , and shear modulus G was considered. To obtain the properties of this model, a linkage between the molecular mechanics and the density functional theory is constructed [Ansari et al. 2015]. The required properties of the beam element are given in Table 1.

3. Calculation of elastic moduli

3.1. Young's modulus. The Young's modulus of a material is the ratio of normal stress to normal strain as obtained from a uniaxial tension test ($E = \sigma/\varepsilon$). Therefore, the Young's modulus of BNNT is calculated using the following equation:

$$E = \frac{FL}{\delta L A_0}, \quad (2)$$

where F is applied force to nanotube, A_0 is the cross-sectional area, and L is the initial length. The longitudinal displacement of the nanotube δL is determined from FE analysis. A_0 is equal to $\pi D t$,

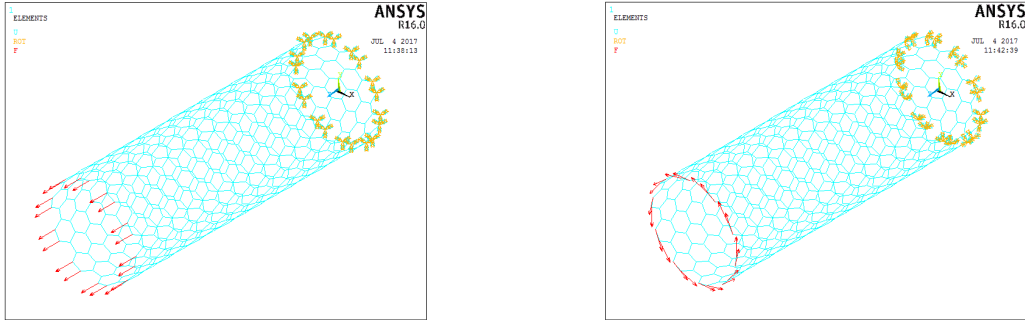


Figure 2. FE meshes of the (10, 10) nanotube with length 40 Å along with the applied loading and boundary conditions: (left) tension, (right) torsion.

where D is the mean diameter of the tube and t is the nanotube thickness. The wall thickness of BNNTs has not yet been clearly specified. The wall thickness is selected as 0.34 nm [Zhi et al. 2005] and the centre of the BNNT wall is placed at the midsection of the tube thickness.

In order to apply the conditions of tension, the nodes of the upper end of the BNNT have been fully built-in (zero displacement and rotation conditions), while the nodes of the bottom end, are subjected to tensile forces [Fereidoon et al. 2014]; see Figure 2 (left).

3.2. Shear modulus. The following relation is used for calculating the shear modulus of BNNTs:

$$G = \frac{TL}{J\theta}, \quad (3)$$

where T stands for the torque acting at the one end of the nanotube and applied by tangential forces. Here, θ and J are torsional angle and polar moment of inertia of the cross-sectional area of the BNNT, respectively. The torsional angle θ is calculated by FE analysis. J is computed by (4), considering the BNNT as a hollow tube with middiameter D and thickness t :

$$J = \frac{1}{32}\pi[(D+t)^4 - (D-t)^4]. \quad (4)$$

In order to apply the conditions of torsion, the nodes of the upper end of the BNNT are fully built-in (zero displacement and rotation conditions), while the nodes of the bottom end are subjected to tangential forces; see Figure 2 (right).

4. Results and discussions

The mechanical properties of BNNTs depend on their length, chirality, diameter, and defect. Several works investigated the dependence of the elastic moduli of BNNTs on their diameter and chirality. Arm-chair and zig-zag nanotubes are included in the investigation.

4.1. Elastic moduli of BNNT and defected BNNT. The elastic properties of BNNTs depend on their size and chirality. In this section, the FE model is applied to investigate the effect of chirality on the elastic moduli of regular BNNTs and defected ones. For modelling defective nanotubes, three bonds of each nanotube are omitted. Loading and boundary conditions of defected (10, 10) BNNTs with length of 40 Å in tension and torsion states are shown in Figure 3 (left) and Figure 3 (right), respectively.

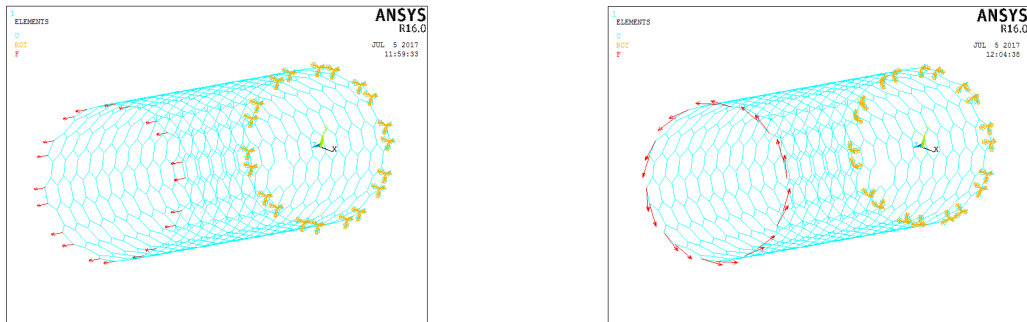


Figure 3. FE meshes of the (10, 10) defected nanotube with length 40 Å along with the applied loading and boundary conditions: (left) tension, (right) torsion.

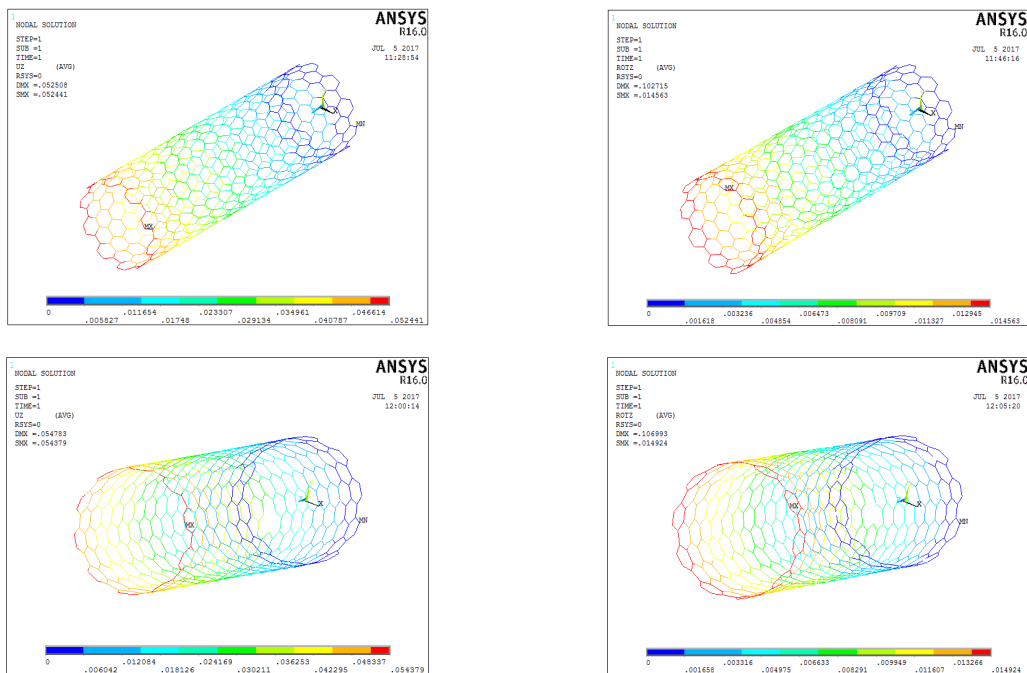


Figure 4. Deformations of a regular nanotube (top) and a defected one (bottom) under tension (left column) and torsion (right column) loading.

Deformations of nanotubes and defected nanotubes under tension and torsion loading are represented in Figure 4. As shown in Figure 4, the longitudinal and angular deformations of defected nanotubes were more pronounced than in regular nanotubes. Figure 5 shows the comparisons of the Young's and shear moduli of regular BNNTs and defected ones with length 40 Å in terms of chirality. Results show that as the chirality increases, the Young's modulus and shear modulus of the BNNT increases but the increase in Young's modulus is not considerable. The mechanical properties of the defected nanotube were lower than the nanotube with the same chirality. Also, as the chirality increases, the elastic moduli of defected BNNT increases.

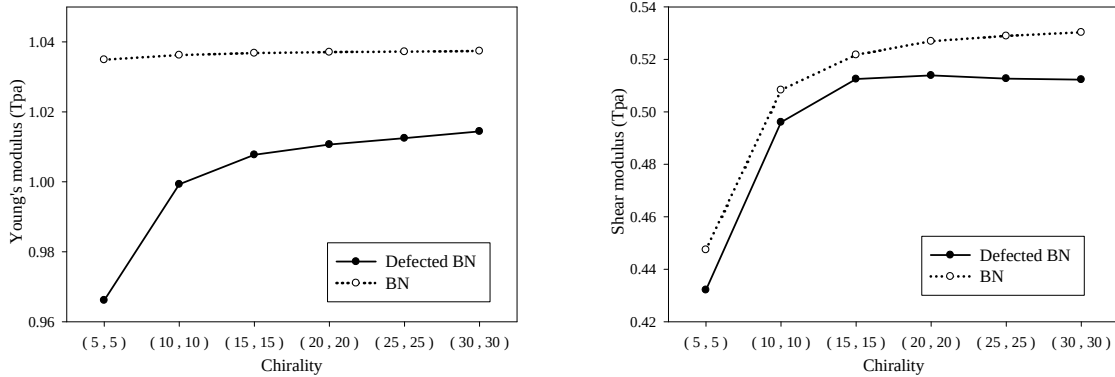


Figure 5. The elastic moduli of a regular nanotube and a defected one plotted against the chirality for $L = 40 \text{ \AA}$.

| elastic moduli | (TPa) | reference |
|-----------------|-------------------------|-------------------------------------|
| Young's modulus | 1.22 ± 0.24 | [Chopra and Zettl 1998] |
| | 1.022–1.112 | [Fereidoon et al. 2015] |
| | 0.71–0.83 | [Zhi et al. 2010] |
| | 0.862–0.94 | [Verma et al. 2007] |
| | 0.982–1.11 | [Hernández et al. 1999] |
| | 0.895 | [Fakhrabad and Shahtahmassebi 2013] |
| | 0.7–1.2 | [Santosh et al. 2009] |
| | 0.7–1.2 | [Bettinger et al. 2002] |
| | 1.1–1.3 | [Wei et al. 2010] |
| | 0.764–0.821 | [Suryavanshi et al. 2004] |
| | 0.7–0.9 | [Zhong et al. 2001] |
| 1 | [Chowdhury et al. 2010] | |
| | 1.034–1.037 | current work |
| shear modulus | 0.42 | [Chowdhury et al. 2010] |
| | 0.44–0.53 | current work |

Table 2. Elastic moduli of BNNTs from simulation and experimental works.

The Young's and shear moduli of BNNTs are archived by tension and torsion loading in the range of 1.039 TPa–1.041 TPa and 0.44 TPa–0.52 TPa, respectively. Elastic moduli of BNNT from simulation and experimental works are given in Table 2. The current results are in good agreement with simulated and experimental values.

4.2. Young's modulus. Zigzag nanotubes with chirality (5, 0), (10, 0), (15, 0), (20, 0), (25, 0), and (30, 0) and armchair nanotubes with chirality (5, 5), (10, 10), (15, 15), (20, 20), (25, 25), and (30, 30) were analysed under tension forces. The BNNTs have lengths of 40 Å, 60 Å, 80 Å, and 100 Å. The effects of chirality, length, and radius on the Young's moduli of BNNTs are investigated in the following:

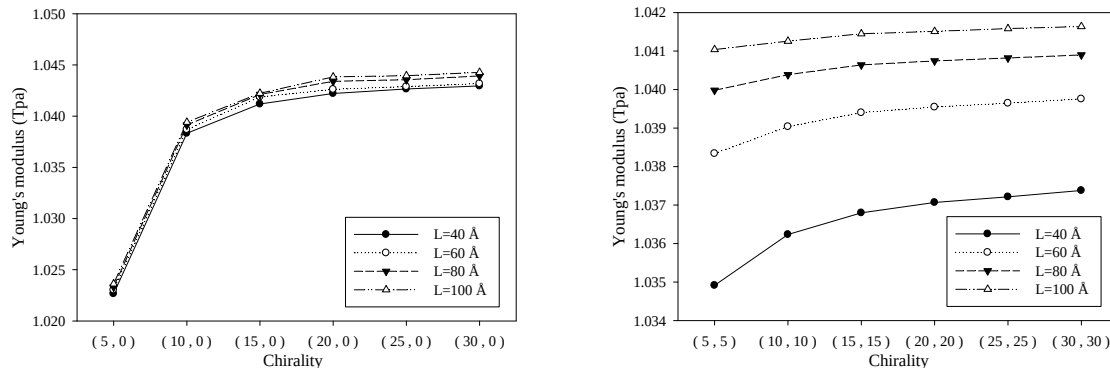


Figure 6. Young's modulus of BNNTs as a function of chirality: (left) zigzag, (right) armchair.

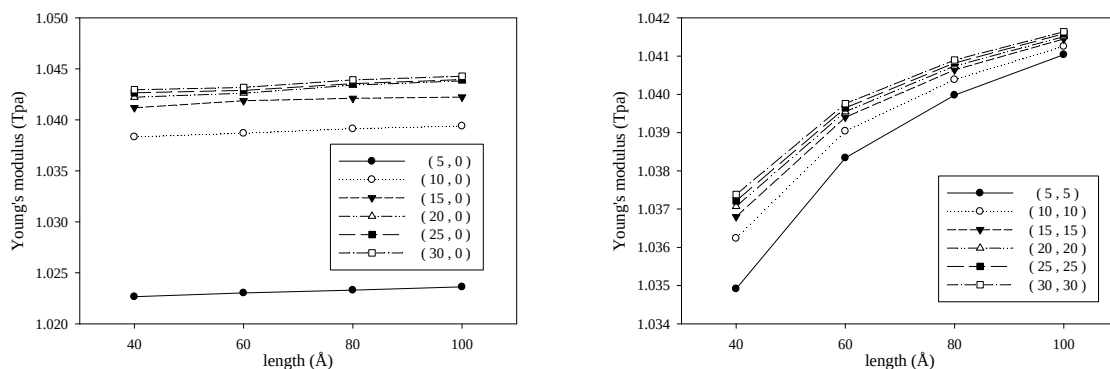


Figure 7. Young's modulus of BNNTs as a function of length: (left) zigzag, (right) armchair.

Chirality. Figures 6 (left) and 6 (right) indicate the variation of Young's modulus of zigzag and armchair nanotubes (respectively) with lengths of 40 \AA , 60 \AA , 80 \AA , and 100 \AA as a function of chirality. For armchair and zigzag nanotubes, with increasing chirality and consequently radius, the Young's modulus increases. The gradients of variations are greater in small radii, and with increasing radius, the Young's modulus tends to constant values. Moreover, the Young's moduli of zigzag nanotubes with different lengths are very close, but in armchair nanotubes, the differences are significant.

Length. Variations of Young's modulus of zigzag and armchair nanotubes with respect to length are plotted in Figures 7 (left) and 7 (right), respectively. For armchair and zigzag nanotubes, with increasing length, the Young's modulus increases. The gradients of variations become smaller as the length increases, and tend to constant values. Furthermore, the changes of Young's moduli of zigzag BNNTs with respect to lengths aren't considerable when compared to armchair ones.

Radius. Armchair and zigzag nanotubes are arranged in terms of increasing nanotube radius and are represented in Table 3. Young's moduli of armchair and zigzag nanotubes in terms of radius for different lengths is shown in Figure 8. Generally, with an increase in radius, the Young's modulus of BNNTs increases. But for roughly similar radii, the Young's moduli of zigzag nanotubes are larger than for armchair nanotubes. For example, the radius of the nanotube (10, 10) lies between the radii of the nanotubes (15, 0) and (20, 0), but its Young's modulus is less than the two other BNNTs.

| chirality | radius | chirality | radius |
|-----------|--------|-----------|--------|
| (5, 0) | 1.999 | (25, 0) | 9.993 |
| (5, 5) | 3.462 | (15, 15) | 10.385 |
| (10, 0) | 3.997 | (30, 0) | 11.991 |
| (15, 0) | 5.996 | (20, 20) | 13.846 |
| (10, 10) | 6.923 | (25, 25) | 17.308 |
| (20, 0) | 7.994 | (30, 30) | 20.77 |

Table 3. Arranging armchair and zigzag nanotubes in terms of increasing radius.

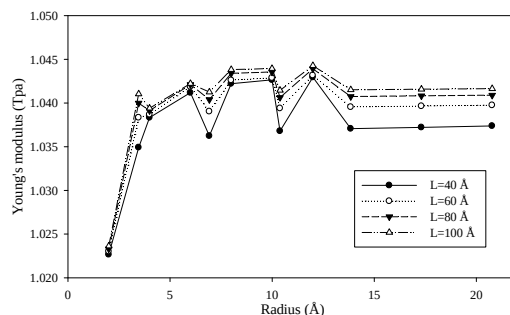


Figure 8. Young's modulus of zigzag and armchair BNNTs as a function of radius.

4.3. Shear modulus. Zigzag nanotubes with chirality (5, 0), (10, 0), (15, 0), (20, 0), (25, 0), and (30, 0) and armchair nanotubes with chirality (5, 5), (10, 10), (15, 15), (20, 20), (25, 25), and (30, 30) were analysed under torsion forces (torque). BNNTs with different lengths of 40 Å, 60 Å, 80 Å, and 100 Å were studied. The influences of chirality, length, and radius on the shear modulus of BNNTs were studied and results are given in the following:

Chirality. Figures 9 (left) and 9 (right) illustrate the variations of shear moduli of zigzag and armchair nanotubes with lengths of 40 Å, 60 Å, 80 Å, and 100 Å in terms of chirality. As the chirality increases, and subsequently as the radii of the zigzag and armchair nanotubes increase, their shear moduli increase. The slope of the changes in the smaller radii is greater and reaches a constant value as the radius increases. Furthermore, the shear moduli of armchair-type nanotubes are larger than the zigzag and increase as the chirality increases. As chirality increases, the shear moduli of armchair and zigzag nanotubes approximately reach equal constant value.

Length. Shear moduli of zigzag and armchair nanotubes with respect to length are plotted in Figure 10, left and right, respectively. Figure 10 indicates that as the length of zigzag and armchair BNNTs increases, the shear modulus decreases. The gradients of variations reduce with increasing length and tend to constant values. The results show that the mechanical properties of BNNTs depend on chirality and the length of the nanotubes.

Radius. Shear moduli of armchair and zigzag nanotubes in terms of radius for different lengths is plotted in Figure 11. In general, with increasing radius, the BNNT shear modulus increases. But for roughly similar radii, the moduli of zigzag nanotubes is larger than the armchair ones.

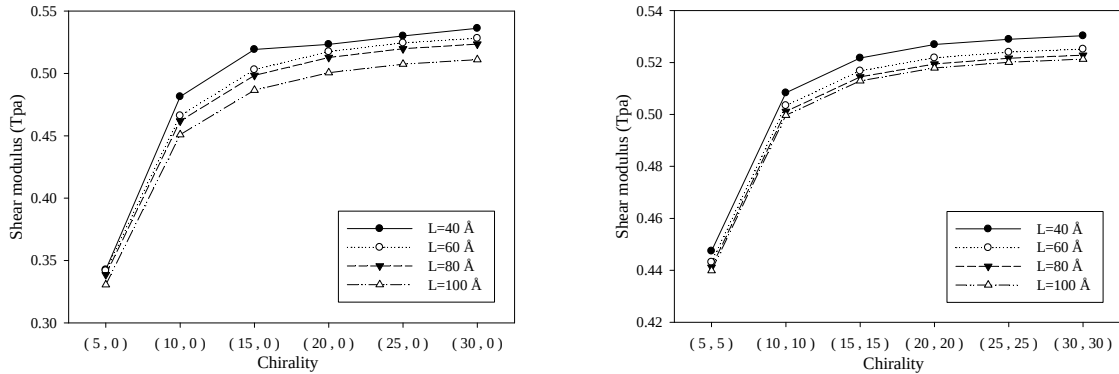


Figure 9. Shear modulus of BNNTs as a function of chirality: (left) zigzag, (right) armchair.

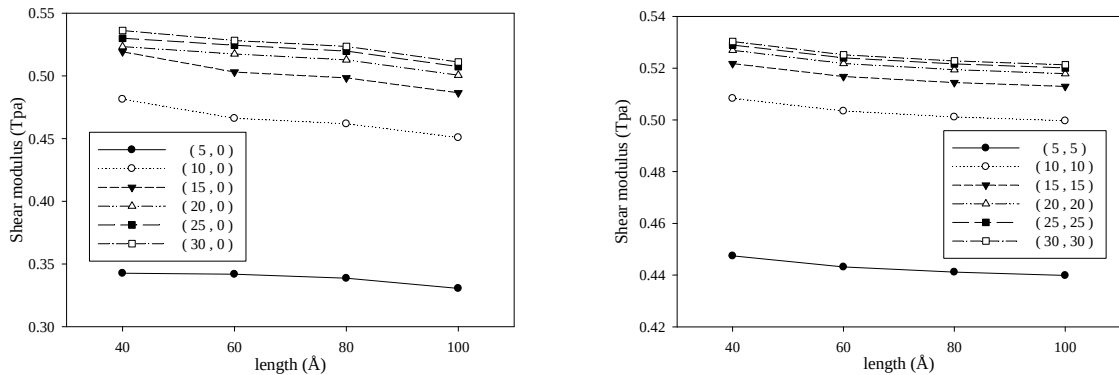


Figure 10. Shear modulus of BNNTs as a function of length: (left) zigzag, (right) armchair.

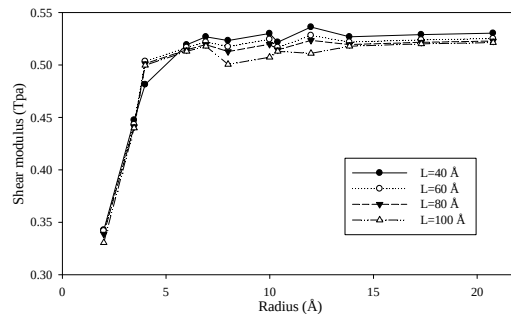


Figure 11. Shear modulus of zigzag and armchair BNNTs as a function of radius.

5. Conclusions

Three-dimensional finite element (FE) models for BNNTs have been proposed. To create the FE models, nodes are placed at the locations of atoms and the bonds between them are modelled using three-dimensional elastic beam elements via considering a linkage between molecular and continuum mechanics. The FE model comprises a small number of elements and performs with minimal computational time

and minimal computational power. This advantage, in combination with the modelling abilities of the FE method, extends the model applicability to all kinds of nanotubes with very large numbers of atoms.

The results showed that defection of nanotube decreases the mechanical properties. The effects of chirality, length, and radius on Young's modulus and shear modulus of armchair and zigzag BNNTs were investigated based on the FE model. The values of the Young's modulus and shear modulus of BNNTs without defects have changed from 1.022 TPa to 1.042 TPa and from 0.33 TPa to 0.536 TPa, respectively.

Results show that with increasing chirality, and consequently radius, the Young's modulus and shear modulus increase. As the length of zigzag and armchair BNNTs increases, the Young's modulus increases and the shear modulus decreases. Generally, as the radius increases, the Young's modulus and shear modulus increase. Furthermore, in a roughly similar radius, generally, the elastic moduli of zigzag nanotubes are larger than the armchair ones. Hence, the elastic moduli of BNNTs, especially at low radii and lengths, depend on the chirality (atomic arrangement) and the length of the nanotubes.

Also, it was observed that by using the FEM based on molecular dynamics, one can accurately determine the mechanical properties of the BNNTs. Due to the mechanical properties, BNNTs can be applied as a suitable substitute for CNTs in combination with polymers to produce specific nanocomposites.

References

- [Akdim et al. 2003] B. Akdim, R. Pachter, X. Duan, and W. W. Adams, "Comparative theoretical study of single-wall carbon and boron-nitride nanotubes", *Phys. Rev. B* **67**:24 (2003), 245404.
- [Ansari et al. 2015] R. Ansari, S. Rouhi, M. Mirnezhad, and M. Aryayi, "Stability characteristics of single-walled boron nitride nanotubes", *Archiv. Civil Mech. Eng.* **15** (2015), 162–170.
- [Bahrami Panah and Vaziri 2015] N. Bahrami Panah and R. Vaziri, "Structure and electronic properties of single-walled zigzag BN and $B_3C_2N_3$ nanotubes using first-principles methods", *Int. J. Nano Dimen.* **6**:2 (2015), 157–165.
- [Bettinger et al. 2002] H. F. Bettinger, T. Dumitrică, G. E. Scuseria, and B. I. Yakobson, "Mechanically induced defects and strength of BN nanotubes", *Phys. Rev. B* **65**:4 (2002), 041406.
- [Chang and Gao 2003] T. C. Chang and H. J. Gao, "Size-dependent elastic properties of a single-walled carbon nanotube via a molecular mechanics model", *J. Mech. Phys. Solids* **51** (2003), 1059.
- [Chang et al. 2005] C. W. Chang, W. Q. Han, and A. Zettl, "Thermal conductivity of B-C-N and BN nanotubes", *Appl. Phys. Lett.* **86** (2005), 173102.
- [Chen et al. 2004a] C.-W. Chen, M.-H. Lee, and S. J. Clark, "Band gap modification of single-walled carbon nanotube and boron nitride nanotube under a transverse electric field", *Nanotechnology* **15**:12 (2004), 1837.
- [Chen et al. 2004b] Y. Chen, J. Zou, S. J. Campbell, and G. L. Caer, "Boron nitride nanotubes: pronounced resistance to oxidation", *Appl. Phys. Lett.* **84** (2004), 2430–2432.
- [Chopra and Zettl 1998] N. G. Chopra and A. Zettl, "Measurement of the elastic modulus of a multi-wall boron nitride nanotube", *Solid State Comm.* **105**:5 (1998), 297–300.
- [Chopra et al. 1995] N. G. Chopra, R. J. Luyken, K. Cherrey, V. H. Crespi, M. L. Cohen, S. G. Louie, and A. Zettl, "Boron nitride nanotubes", *Science* **269**:5226 (1995), 966–967.
- [Chowdhury et al. 2010] R. Chowdhury, C. Y. Wang, S. Adhikari, and F. Scarpa, "Vibration and symmetry-breaking of boron nitride nanotubes", *Nanotechnology* **21**:36 (2010), 365702.
- [Fakhrabad and Shahtahmassebi 2013] D. V. Fakhrabad and N. Shahtahmassebi, "First-principles calculations of the Young's modulus of double wall boron-nitride nanotubes", *Mater. Chem. Phys.* **138**:2 (2013), 963–966.
- [Fereidoon et al. 2014] A. Fereidoon, M. Rajabpour, and H. Hemmatian, "Elastic moduli of carbon nanotubes with new geometry based on FEM", *J. Theor. Appl. Mech. (Warsaw)* **52**:1 (2014), 235–245.

- [Fereidoon et al. 2015] A. Fereidoon, M. Mostafaei, M. D. Ganji, and F. Memarian, "Atomistic simulations on the influence of diameter, number of walls, interlayer distance and temperature on the mechanical properties of BNNTs", *Superlatt. Microstruct.* **86** (2015), 126–133.
- [Golberg et al. 1999] D. Golberg, Y. Bando, W. Han, K. Kurashima, and T. Sato, "Single-walled B-doped carbon, B/N-doped carbon and BN nanotubes synthesized from single-walled carbon nanotubes through a substitution reaction", *Chem. Phys. Lett.* **208**:3 (1999), 337–342.
- [Golberg et al. 2001] D. Golberg, Y. Bando, K. Kurashima, and T. Sato, "Synthesis and characterization of ropes made of BN multiwalled nanotubes", *Scr. Mater.* **44**:8 (2001), 1561–1565.
- [Golberg et al. 2007] D. Golberg, P. M. F. J. Costa, O. Lourie, M. Mitome, X. Bai, K. Kurashima, C. Zhi, C. Tang, and Y. Bando, "Direct force measurements and kinking under elastic deformation of individual multiwalled boron nitride nanotubes", *Nano Lett.* **7**:7 (2007), 2146–2151.
- [Griebel and Hamaekers 2007] M. Griebel and J. Hamaekers, "Molecular dynamics simulations of boron-nitride nanotubes embedded in amorphous Si-BN", *Comput. Mater. Sci.* **39**:3 (2007), 502–517.
- [Griebel et al. 2009] M. Griebel, J. Hamaekers, and F. Heber, "A molecular dynamics study on the impact of defects and functionalization on the Young modulus of boron-nitride nanotubes", *Comput. Mater. Sci.* **45**:4 (2009), 1097–1103.
- [Hemmatian et al. 2014] H. Hemmatian, A. Fereidoon, and M. Rajabpour, "Mechanical properties investigation of defected, twisted, elliptic, bended and hetero-junction carbon nanotubes based on FEM", *Fullerenes, Nanotubes and Carbon Nanostructures* **22** (2014), 528–544.
- [Hernández et al. 1998] E. Hernández, C. Goze, P. Bernier, and A. Rubio, "Elastic properties of C and $B_xC_yN_z$ composite nanotubes", *Phys. Rev. Lett.* **80**:20 (1998), 4502–4505.
- [Hernández et al. 1999] E. Hernández, C. Goze, P. Bernier, and A. Rubio, "Elastic properties of single-wall nanotubes", *Appl. Phys. A* **68** (1999), 287–292.
- [Ishigami et al. 2005] M. Ishigami, J. D. Sau, S. Aloni, M. L. Cohen, and A. Zettl, "Observation of the giant Stark effect in boron-nitride nanotubes", *Phys. Rev. Lett.* **94**:5 (2005), 056804.
- [Khaleghian and Azarakhshi 2016] M. Khaleghian and F. Azarakhshi, "Electronic properties studies of benzene under boron nitride nano ring field", *Int. J. Nano Dimen.* **7**:4 (2016), 290–294.
- [Khoo et al. 2004] K. H. Khoo, M. S. C. Mazzoni, and S. G. Louie, "Tuning the electronic properties of boron nitride nanotubes with transverse electric fields: a giant dc Stark effect", *Phys. Rev. B* **69**:20 (2004), 201401.
- [Li and Chou 2003] C. Li and T.-W. Chou, "A structural mechanics approach for the analysis of carbon nanotubes", *Int. J. Solids Struct.* **40**:10 (2003), 2487–2499.
- [Li and Chou 2006] C. Li and T.-W. Chou, "Static and dynamic properties of single-walled boron nitride nanotubes", *J. Nanosci. Nanotechnol.* **6**:1 (2006), 54–60.
- [Loiseau et al. 1996] A. Loiseau, F. Willaime, N. Demoncey, G. Hug, and H. Pascard, "Boron nitride nanotubes with reduced numbers of layers synthesized by arc discharge", *Phys. Rev. Lett.* **76**:25 (1996), 4737–4740.
- [Lu 1997] J. P. Lu, "Elastic properties of carbon nanotubes and nanoropes", *Phys. Rev. Lett.* **97**:7 (1997), 1297.
- [Mehar and Panda 2017] K. Mehar and S. K. Panda, "Elastic bending and stress analysis of carbon nanotube-reinforced composite plate: experimental, numerical, and simulation", *Adv. Polym. Technol.* (2017), 1–15.
- [Mehar et al. 2017a] K. Mehar, S. K. Panda, T. Q. Bui, and T. R. Mahapatra, "Nonlinear thermoelastic frequency analysis of functionally graded CNT-reinforced single/doubly curved shallow shell panels by FEM", *J. Therm. Stresses* **40**:7 (2017), 899–916.
- [Mehar et al. 2017b] K. Mehar, S. K. Panda, and T. R. Mahapatra, "Theoretical and experimental investigation of vibration characteristic of carbon nanotube reinforced polymer composite structure", *Int. J. Mech. Sci.* **133** (2017), 319–329.
- [Mehar et al. 2017c] K. Mehar, S. K. Panda, and B. K. Patle, "Stress, deflection, and frequency analysis of CNT reinforced graded sandwich plate under uniform and linear thermal environment: a finite element approach", *Polym. Compos.* (2017).
- [Mehar et al. 2017d] K. Mehar, S. K. Panda, and B. K. Patle, "Thermoelastic vibration and flexural behavior of FG-CNT reinforced composite curved panel", *Int. J. Appl. Mech.* **9**:4 (2017), 1750046.

- [Mehar et al. 2018] K. Mehar, S. K. Panda, and T. R. Mahapatra, "Large deformation bending responses of nanotube-reinforced polymer composite panel structure: numerical and experimental analyses", *Proceedings of the Institution of Mechanical Engineers, Part G: Journal of Aerospace Engineering* (2018), 0954410018761192.
- [Mirzaei and Salamat Ahangari 2016] M. Mirzaei and R. Salamat Ahangari, "Density functional explorations of quadrupole coupling constants for BN, BP, AlN, and AlP graphene-like structures", *Int. J. Nano Dimen.* **7**:4 (2016), 284–289.
- [Molani 2017] F. Molani, "The effect of C, Si, N, and P impurities on structural and electronic properties of armchair boron nanotube", *J. Nanostruct. Chem.* **7**:3 (2017), 243–248.
- [Odegard et al. 2002] G. M. Odegard, T. S. Gates, L. M. Nicholson, and K. E. Wise, "Equivalent continuum modelling of nano-structured materials", *Compos. Sci. Technol.* **62** (2002), 1869.
- [Rubio et al. 1994] A. Rubio, J. L. Corkill, and M. L. Cohen, "Theory of graphitic boron nitride nanotubes", *Phys. Rev. B* **49**:7 (1994), 5081–5084.
- [Sánchez-Portal et al. 1999] D. Sánchez-Portal, E. Artacho, J. M. Soler, A. Rubio, and P. Ordejón, "Ab initio structural, elastic, and vibrational properties of carbon nanotubes", *Phys. Rev. B* **59**:19 (1999), 12678–12688.
- [Santosh et al. 2009] M. Santosh, P. K. Maiti, and A. Sood, "Elastic properties of boron nitride nanotubes and their comparison with carbon nanotubes", *J. Nanosci. Nanotechnol.* **9**:9 (2009), 5425–5430.
- [Suryavanshi et al. 2004] A. P. Suryavanshi, M. Yu, J. Wen, C. Tang, and Y. Bando, "Elastic modulus and resonance behaviour of boron nitride nanotubes", *Appl. Phys. Lett.* **84**:14 (2004), 2527–2529.
- [Terrones et al. 1996] M. Terrones, W. K. Hsu, H. Terrones, J. P. Zhang, S. Ramos, J. P. Hare, R. Castillo, K. Prassides, A. K. Cheetham, H. W. Kroto, and D. R. M. Walton, "Metal particle catalysed production of nanoscale BN structures", *Chem. Phys. Lett.* **259**:5 (1996), 568–573.
- [Vaccarini et al. 2000] L. Vaccarini, C. Goze, L. Henrard, E. Hernández, P. Bernier, and A. Rubio, "Mechanical and electronic properties of carbon and boron-nitride nanotubes", *Carbon* **38**:11-12 (2000), 1681–1690.
- [Verma et al. 2007] V. Verma, V. Jindal, and K. Dharamvir, "Elastic moduli of a boron nitride nanotube", *Nanotechnology* **18**:43 (2007), 435711.
- [Wei et al. 2010] X. Wei, M. S. Wang, Y. Bando, and D. Golberg, "Tensile tests on individual multi-walled boron nitride nanotubes", *Adv. Mater.* **22**:43 (2010), 4895–4899.
- [Wu et al. 2004] X. Wu, J. Yang, J. G. Hou, and Q. Zhu, "Deformation-induced site selectivity for hydrogen adsorption on boron nitride nanotubes", *Phys. Rev. B* **69**:15 (2004), 153411.
- [Yakobson et al. 1996] B. I. Yakobson, C. J. Brabec, and J. Bernholc, "Nanomechanics of carbon tubes: instabilities beyond linear range", *Phys. Rev. Lett.* **76** (1996), 2511.
- [Zhi et al. 2005] C. Zhi, Y. Bando, C. Tang, and D. Golberg, "Immobilization of proteins on boron nitride nanotubes", *J. Am. Chem. Soc.* **127**:49 (2005), 17144–17145.
- [Zhi et al. 2010] C. Zhi, Y. Bando, C. Tang, and D. Golberg, "Boron nitride nanotubes", *Mater. Sci. Eng. R* **70** (2010), 92–111.
- [Zhong et al. 2001] D. Y. Zhong, S. Liu, G. Y. Zhang, and E. G. Wang, "Large-scale well aligned carbon nitride nanotube films: low temperature growth and electron field emission", *J. Appl. Phys.* **89** (2001), 5939.

Received 27 Jan 2018. Revised 25 Apr 2018. Accepted 9 May 2018.

HOSSEIN HEMMATIAN: hoseinhemmatian@gmail.com

Department of Mechanical Engineering, Semnan Branch, Islamic Azad University, Semnan, Iran

MOHAMMAD REZA ZAMANI: a_mrzamani@mut.ac.ir

Faculty of Mechanical Engineering, Malek-Ashtar University of Technology, Tehran, Iran

JAFAR ESKANDARI JAM: eskandari@mut.ac.ir

Faculty of Mechanical Engineering, Malek-Ashtar University of Technology, Tehran, Iran

JOURNAL OF MECHANICS OF MATERIALS AND STRUCTURES

msp.org/jomms

Founded by Charles R. Steele and Marie-Louise Steele

EDITORIAL BOARD

| | |
|-----------------------|--|
| ADAIR R. AGUIAR | University of São Paulo at São Carlos, Brazil |
| KATIA BERTOLDI | Harvard University, USA |
| DAVIDE BIGONI | University of Trento, Italy |
| MAENGHYO CHO | Seoul National University, Korea |
| HUILING DUAN | Beijing University |
| YIBIN FU | Keele University, UK |
| IWONA JASIUK | University of Illinois at Urbana-Champaign, USA |
| DENNIS KOCHMANN | ETH Zurich |
| MITSUTOSHI KURODA | Yamagata University, Japan |
| CHEE W. LIM | City University of Hong Kong |
| ZISHUN LIU | Xi'an Jiaotong University, China |
| THOMAS J. PENCE | Michigan State University, USA |
| GIANNI ROYER-CARFAGNI | Università degli studi di Parma, Italy |
| DAVID STEIGMANN | University of California at Berkeley, USA |
| PAUL STEINMANN | Friedrich-Alexander-Universität Erlangen-Nürnberg, Germany |
| KENJIRO TERADA | Tohoku University, Japan |

ADVISORY BOARD

| | |
|---------------|---|
| J. P. CARTER | University of Sydney, Australia |
| D. H. HODGES | Georgia Institute of Technology, USA |
| J. HUTCHINSON | Harvard University, USA |
| D. PAMPLONA | Universidade Católica do Rio de Janeiro, Brazil |
| M. B. RUBIN | Technion, Haifa, Israel |

PRODUCTION production@msp.org

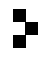
SILVIO LEVY Scientific Editor

See msp.org/jomms for submission guidelines.

JoMMS (ISSN 1559-3959) at Mathematical Sciences Publishers, 798 Evans Hall #6840, c/o University of California, Berkeley, CA 94720-3840, is published in 10 issues a year. The subscription price for 2018 is US \$615/year for the electronic version, and \$775/year (+\$60, if shipping outside the US) for print and electronic. Subscriptions, requests for back issues, and changes of address should be sent to MSP.

JoMMS peer-review and production is managed by EditFLOW[®] from Mathematical Sciences Publishers.

PUBLISHED BY

 **mathematical sciences publishers**
nonprofit scientific publishing

<http://msp.org/>

© 2018 Mathematical Sciences Publishers

Journal of Mechanics of Materials and Structures

Volume 13, No. 3

May 2018

-
- Formulas for the H/V ratio of Rayleigh waves in compressible prestressed hyperelastic half-spaces** PHAM CHI VINH, THANH TUAN TRAN, VU THI NGOC ANH and LE THI HUE 247
- Geometrical nonlinear dynamic analysis of tensegrity systems via the corotational formulation** XIAODONG FENG 263
- Shaft-hub press fit subjected to couples and radial forces: analytical evaluation of the shaft-hub detachment loading** ENRICO BERTOCCHI, LUCA LANZONI, SARA MANTOVANI, ENRICO RADI and ANTONIO STROZZI 283
- Approximate analysis of surface wave-structure interaction** NIHAL EGE, BARIŞ ERBAŞ, JULIUS KAPLUNOV and PETER WOOTTON 297
- Tuning stress concentrations through embedded functionally graded shells** XIAOBAO LI, YIWEI HUA, CHENYI ZHENG and CHANGWEN MI 311
- Circular-hole stress concentration analysis on glass-fiber-cotton reinforced MC-nylon** YOU RUI TAO, NING RUI LI and XU HAN 337
- Elastic moduli of boron nitride nanotubes based on finite element method** HOSSEIN HEMMATIAN, MOHAMMAD REZA ZAMANI and JAFAR ESKANDARI JAM 351
- Effect of interconnect linewidth on the evolution of intragranular microcracks due to surface diffusion in a gradient stress field and an electric field** LINYONG ZHOU, PEIZHEN HUANG and QIANG CHENG 365
- Uncertainty quantification and sensitivity analysis of material parameters in crystal plasticity finite element models** MIKHAIL KHADYKO, JACOB STURDY, STEPHANE DUMOULIN, LEIF RUNE HELLEVIK and ODD STURE HOPPERSTAD 379
- Interaction of shear cracks in microstructured materials modeled by couple-stress elasticity** PANOS A. GOURGIOTIS 401



1559-3959(2018)13:3;1-Z